Title

Direct Phase Equilibrium Simulations of NIPAM Oligomers in Water

Journal

The Journal of Physical Chemistry B, 120(13)

ISSN

1520-6106

Authors

Boţan, Vitalie
Ustach, Vincent
Faller, Roland
et al.

Publication Date

2016-04-07

DOI

10.1021/acs.jpcb.6b00228

Peer reviewed

Direct Phase Equilibrium Simulations of NIPAM Oligomers in Water

Vitalie Boţan,[†] Vincent Ustach,[‡] Roland Faller,[‡] and Kai Leonhard[*,†]

Lehrstuhl für Technische Thermodynamik, RWTH Aachen University, Schinkelstr. 8, 52062 Aachen, Germany, and Department of Chemical Engineering and Materials Science, University of California Davis, One Shields Ave, Davis, CA 95616, USA

E-mail: Kai.Leonhard@ltt.rwth-aachen.de

Phone: +49 (0)241 8098174. Fax: +49 (0)241 8092255

KEYWORDS: MD force fields; LCST; Lower critical solution temperature; Polymer solubility; Slow dynamics

[*]To whom correspondence should be addressed

[†]Lehrstuhl für Technische Thermodynamik, RWTH Aachen University, Schinkelstr. 8, 52062 Aachen, Germany

[‡]Department of Chemical Engineering and Materials Science, University of California Davis, One Shields Ave, Davis, CA 95616, USA

Abstract

NIPAM (N–isopropyl acrylamide)–based polymers in water show many interesting properties in experiments, including a lower critical solution temperature (LCST) at 305 K and a conformational transition of single chains at the same temperature. The results of many simulation studies suggest that standard force–fields are able to describe the conformational transition and the phase equilibrium well. We show by performing long molecular dynamics simulations of the direct liquid–liquid phase equilibrium of NIPAM trimers in water that there is no LCST in the expected temperature range for any of the force–fields under study. The results show further that the relaxation times of single–chain simulations are considerably longer than anticipated. Conformational transitions of single polymers can therefore not necessarily be used as surrogates for a real phase transition.

Introduction

Thermoresponsive materials are an interesting class of materials with wide–spread applications, e.g. in catalysis, sensors, enzyme encapsulation, and drug delivery.[1,2] One of the best–studied materials of this class is poly–N–isopropyl acryl amide (PNIPAM). This polymer is completely soluble in water below 32°C but phase separates from water above this lower critical solution temperature (LCST). Even more interestingly, PNIPAM is fully soluble in pure methanol but PNIPAM in mixtures of water and methanol with 0–50 mol % methanol exhibits a lower LCST than in pure water. This phenomenon is called cononsolvency. The experimental, theoretical, and simulative work on PNIPAM solutions and PNIPAM–based gels has been reviewed recently.[3]

Atomistic molecular dynamics (MD) simulations of PNIPAM (mostly the oligomeric version which we refer to here as ONIPAM) have been performed frequently to gain a deeper understanding of the mechanisms leading to phase separation or gel collapse using various intermolecular potentials. Due to computational limitations, often the conformational changes of a single chain have been studied and used as a surrogate for the phase equilibrium which clearly is a collaborative effect over many chains. After briefly reviewing the recent simulation work, it is the purpose of the present work to show by explicit simulations of liquid–liquid phase equilibria that the correlation between these phenomena is not as simple as generally assumed in the literature.[4–7] Walter et al. simulated a single PNIPAM 30mer in water using the OPLS–AA,[8,9] GROMOS–96 53A6 (G53A6)[10,11] as well as GROMOS–87 (G87)[12] force fields for the polymer and SPC/E[13] and TIP4P[14] models for water.[4] The authors obtained both a stretched conformation of the single chain below the LCST at 280 K and a collapsed conformation above the LCST at 360 K within the simulation time of 40 ns but only with the following two combinations of force–fields: OPLS–AA + SPC/E and G53A6 + TIP4P. They concluded from these observations that these two combinations describe the studied systems most reasonably.

It is noteworthy that they found a single–chain coil–globule transition which might or

might not be the same as a true phase separation and could change the interpretation of earlier studies to some extent. More critically, however, simulations in the tens of nanoseconds time range are likely too short to observe reliably either conformational or phase transitions, as, e.g., for phase studies of phospholipids in water at similar temperatures regularly hundreds of nanoseconds to several microseconds are needed.[15,16]

Liu et al. studied systems with one or two 25mers starting from different conformations for a short time and compare their data to thermodynamic phase data.[17] Two further studies investigated the effect of chain length on the single–chain transition and found that for the OPLS–AA model (with TIP3P and TIP4P water) at least 11 monomers were needed to obtain a conformational transition.[18,19] In these studies, the simulation times are unusually long (100 – 400 ns) and 2 distinct states, a larger one and a more compact one, were observed for a 30mer at 280 K. However, no information is given on the transition time between the states nor any information that allows an assessment of the relative stability for the observed states.

MD simulations of 12 Dreiding[20] NIPAM chains grafted on a silica surface detected de–swelling in F3C water[21] above the experimental LCST within 15 ns but no change in water content below that temperature[5] which led the authors to conclude that "below which [the LCST] the P(NIPAAm) brush is associated with water molecules stably." Alaghemandi and Spohr studied a single 30mer as well as ten 30mer chains of OPLS–UA[8] PNIPAM in TIP3P–water over 30 ns.[6] In the larger systems, structural indicators (end–to–end distance, number of hydrogen bonds, coordination number) show a stronger dependence on temperature than in the single chain system. They concluded that one 30mer may not be enough to detect the LCST but "For the multiple–chain system, on the other hand, clear signatures of an LCST are detectable in the simulation data." Deshmukh et al. used the GROMOS96 force field[10,11] for simulations of NIPAM and SPC/E water[13] below and above the experimental LCST in ratios determined by experiment. Their results were based on very short simulations (4 ns) at constant mole fractions. Their radial distribution functions changed with

temperature as expected from experiments, and from this they concluded that the critical solution temperature was observed. In a follow–up study, they investigated the same system using PCFF[22,23] to simulate the coil–to–globule transition of 3mers to 30mers.[7] Francis et al. studied the radius of gyration of a 50mer of PNIPAM in water for 4 ns using Amber94[24] and TIP3P[14] water.[25] The radius of gyration decreased above the experimental LCST within the simulation time but not below.

Even though the correspondence of the conformational transition to the phase transition has been shown experimentally for long (1.3×10^7 g/mol) PNIPAM chains,[26] we consider some of the interpretations of short simulations of small systems in the literature at least risky. Therefore, in this work we perform long simulations of a single 30mer chain to investigate the required relaxation times and perform direct phase equilibrium simulations[27] of 80 trimers in 3200 water molecules to test the performance of several potentials to reproduce the experimental LCST behavior.

Methods

Molecular simulations using the OPLS–AA + SPCE and TIP3P, Amber94 + TIP3P, and PCFF force fields have been performed using LAMMPS.[28] All oligomers are syndiotactic. The initial structure was prepared with Moltemplate[29] and VMD tools.[30] The 30mer was placed in a cubic box with linear dimension of 80 Å to ensure the absence of periodic image interactions and solvated in 16900 water molecules at the experimental density with the PACKMOL tool.[31] The energy of the resulting system was minimised using the steepest descent and conjugate gradient algorithms for a total of 5000 steps. After minimisation we performed water equilibration in the NVT ensemble at 300 K for at least 4 ns. The polymer backbone was fully extended and kept rigid during the energy minimisation and subsequent NVT run. After the equilibration phase, the simulations were continued for at least 200 ns at temperatures between 280 and 320 K and 1 bar of pressure, employing the Nose–Hoover

thermostat and barostat with a relaxation time of 500 fs.[32] The heteroatomic Lennard–Jones parameters were determined using the geometric combining rule, and the cutoff for the real–space component of the electrostatic portion of the potential and the van der Waals forces was 10.0 Å. The long–ranged electrostatic and van der Waals interactions were treated using the particle–particle particle–mesh (PPPM)[33] method with an RMS accuracy of 10^{-4}. The bond lengths and the angles of water molecules were constrained using the SHAKE[34] algorithm. The time step was set to 2 fs. During the production phase, the energy and density fluctuations were monitored every 100 fs to ensure there were no energy drifts or significant volume jumps.

The molecular simulations using GROMOS 45A3[35] + SPCE have been performed using GROMACS 5.0.5.[36] Meso and Racemo dimers of NIPAM were prepared with Moltemplate and VMD tools. 125 dimers were placed in a cubic box with linear dimension of 74.45 Å and solvated using GROMACS. The energy of the resulting system was minimised using the steepest descent algorithms until the maximum force on any atom was less than 1000 kJ/mol/nm. After minimisation we performed temperature equilibration in the NVT ensemble at the desired temperature of 280 K or 320 K for 100 ps, followed by NPT equilibration at 1 bar for 100 ps. The production run in the NPT ensemble extended for 20 ns. The velocity rescaling thermostat[37] was used with a relaxation time constant of 0.1 ps. The Parrinello–Rahman barostat[38] maintained the pressure at 1 bar with a relaxation time constant of 2 ps. The cutoff for the real–space component of the electrostatic portion of the potential and the van der Waals forces was 10.0 Å. The long–range electrostatic and van der Waals interactions were treated using the Smooth Particle Mesh Ewald method[39] with an RMS accuracy of 10^{-4}. The bond lengths and the angles of water molecules were constrained using the parallel LINCS algorithm P–LINCS[40] with 4^{th} order expansion of the constraint coupling matrix. The time step was set to 2 fs.

Direct phase equilibrium simulations of the liquid–liquid equilibria (LLE) were carried out in a single cuboidal simulation box with a length in z direction that is three times as long

as in x and y direction. Initial minimisation and thermalization was performed as described above. When the equilibrium density was reached, the simulation was continued as a NVT simulation to produce density histograms along the z axis. We present densities averaged over 3 bins for the polymer density to damp fluctuations. The position of the carbonyl C atom of each monomer and that of the oxygen atom of water are used for the density profiles. Some of the direct phase equilibrium simulations have been performed with a 1 fs time step, e.g. those employing the OPLS-AA model for NIPAM in TIP3P water and all simulations based on PCFF because of its flexible water model. Since the OPLS-AA simulations yielded the same results as those with a 2 fs time step employing the same potential, all other simulations with rigid water have been performed with a 2 fs time step.

Detailed geometry and potential parameter information can be found in the SI.

Voronoi tessellation divides the volume of a system into polyhedral cells, with one cell for each atom. The volume of a cell is defined as all points which are closest to a given atom. For a system with atoms of different sizes, the distance between a point in space and an atom is weighted. Radical weighted tessellation[41] was used, where the distance is defined as

$$d = \sqrt{(x_c - x)^2 + (y_c - y)^2 + (z_c - z)^2} - r_{\mathrm{rad}}^2 \tag{1}$$

where x_c, y_c, and z_c denote the center of the atoms, x, y, and z denote the point in space, and r_{rad} denotes the atom radius. The cells are all in contact, and adjacent cells share one common planar face. The surface area of the contact between adjacent atoms is defined as the area of the common face. Voronoi tessellation was used to examine the contact statistics of the system. The program voro++[42] was used to perform the tessellation for 2000 snapshots of the MD trajectory at 50 ps intervals. The probability of an atom type having contact with another atom type in the system is

$$\langle p_{ab} \rangle = \left\langle \frac{A_{ab}}{A_a^{\mathrm{tot}}} \right\rangle \tag{2}$$

where $\langle . \rangle$ denotes a time average, A_{ab} denotes the sum of the surface area of the faces shared between atom types a and b, and A_a^{tot} denotes the total surface area of the cells of atom type a. The atom types in this system are backbone carbon, backbone hydrogen, isopropyl carbon, isopropyl hydrogen, amide carbon, amide oxygen, amide nitrogen, amide hydrogen, and water. The set of atoms types for b included all 9 types listed above, and the set of atom types for a included the set above except water. The data for p_{ab} is therefore an 8×9 grid. This is called the full Voronoi analysis. A set of data was also created by grouping atom types as backbone atoms (backbone carbon and backbone hydrogen), residue atoms (isopropyl carbon, isopropyl hydrogen, amide carbon, amide oxygen, amide nitrogen, and amide hydrogen), or water. This grouped scheme has for b all three types and for a only backbone atoms and residue atoms, leaving a 2×3 grid. This is called the backbone-residue-water (BRW) Voronoi analysis.

The radii of the particles r_{rad} were defined as half the Lennard–Jones σ values. Since the SPC/E water model has no excluded volume for the hydrogen atoms, water molecules were treated as a single interaction site centered around the oxygen atom. During the calculation of the surface areas for each atom, the faces between first, second, and third bonded neighbors were excluded.

Results and Discussion

Figure 1 shows the dependence of the radius of gyration, R_{g}, of a single PNIPAM 30mer chain in pure water on simulation time for three different temperatures. We find a collapse with a conformational transition time at about 20 ns at 320 K but only at more than 100 ns at 290 K. At 280 K the chain does not collapse in over 300 ns. In previous studies, this has been interpreted as having passed the conformational transition temperature. Strictly speaking, since neither the coil nor the globule change their conformation within 300 ns, no unambiguous conclusion regarding the coil–to–globule transition can be made from these

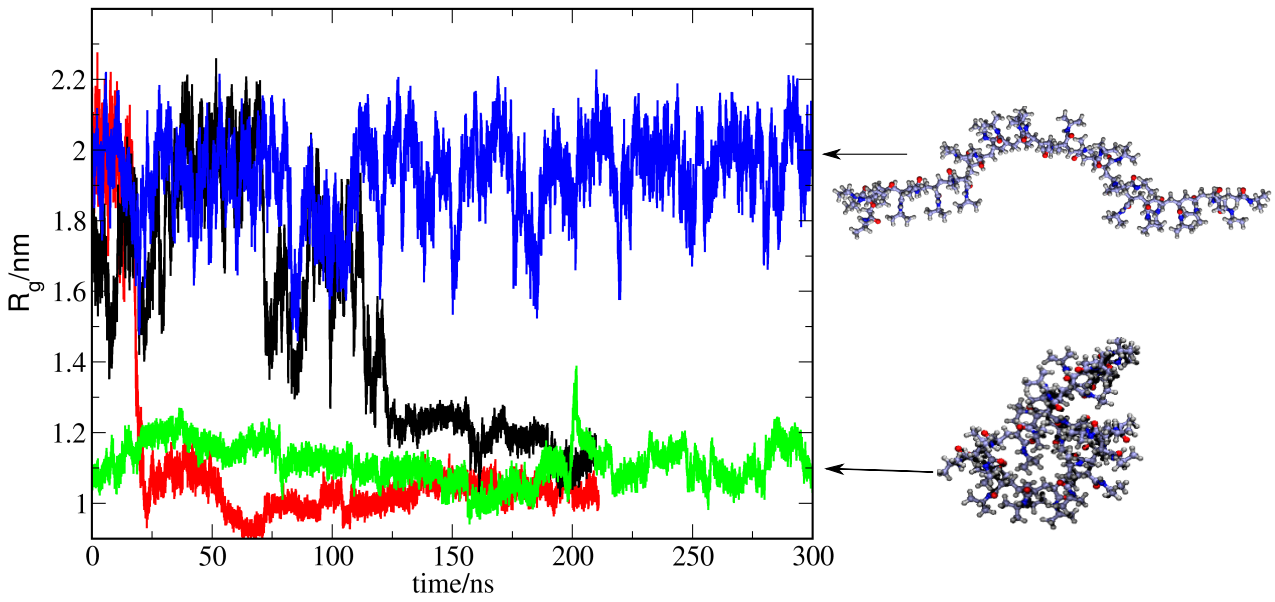

Figure 1: Radius of gyration, R_g, of an OPLS–AA PNIPAM 30mer chain in aqueous solution (16900 SPC/E water molecules) at three temperatures as function of time. Red line: 320 K, black line: 290 K, green and blue lines: 280 K. The simulation shown by the green line started from the conformation of the collapsed chain at 290 K; all others started from the same extended conformation.

data. Therefore, we study further descriptors of the conformational and solvation state of a 30mer first and then the direct phase equilibrium simulations of shorter oligomers. All these results indicate that the temperatures where the coil is the most stable state have not yet been reached, the simulations are just too short to observe a collapse.

Since the radius of gyration does not characterize the solvation state fully, we investigate additional means for its description. As a second means, the contact statistics were analyzed using Voronoi tesselation to reveal information on their solvation states.[41] The atoms groups were defined according to Figure 2. The contact statistics of chemical groups of the 30mers with their environment are shown in Figure 3 for the various states and temperatures. This is the full Voronoi analysis. The analysis creates an 8×9 grid, however Figure 3 shows p_{ab} only for $b = \{$backbone hydrogen, isopropyl hydrogen, water$\}$ to highlight the ab atom pairs with the largest changes in contact over the simulated states. Rather than presenting absolute

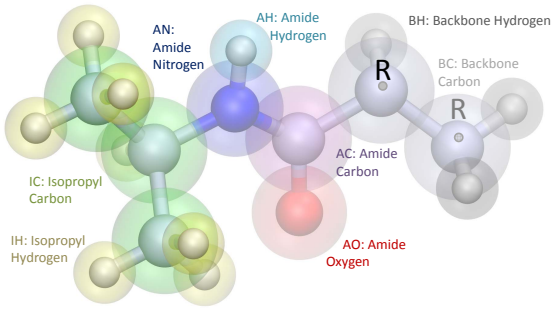

Figure 2: One NIPAM repeat unit with atom group definition for the Voronoi tesselation.

values for p_{ab}, we present the differences between solvation states. The trajectory for the chain in an extended state at 280 K was used as a baseline. The verticle axis of these plots shows $\Delta\langle p_{ab}\rangle = \langle p_{ab}^{T,conf}\rangle - \langle p_{ab}^{280,\text{ext}}\rangle$ where $\langle p_{ab}^{T,conf}\rangle$ represents the average contact statistics between atom type a and atom type b at temperature T and conformation $conf$. A positive value of $\Delta\langle p_{ab}\rangle$ means that in the respective simulation we have more contacts of the ab type than at 280 K extended conformation. For the full 8×9 plots of $\Delta\langle p_{ab}\rangle$, see Figure S1 in SI.

Figure 3a is the difference between extended and compact conformational states of the chain at the same temperature, 280 K. Many atom types have more contact with the nonpolar hydrogens and less contact with water. Figure 3b compares the extended chain at 280 K to the early portion of the trajectory at 290 K when the chain is extended and reveals only slight differences. At the extended state at 290 K the polymer has not significantly shielded itself from water, i.e., there are still significant water–polymer contacts. The extended chain at 290 K collapses after 100–150 ns as characterized by a change in R_g as well as the contact statistics showing a decrease in contacts, Figure 3c, between polymer and water and an increase in hydrophobic group self–interaction contact statistics. The collapsed state at 280 K is more similar to the collapsed state at higher temperatures than to the extended state at 290 K. The difference from 280 K to 320 K, Figure 3d, is more dramatic than from 280 K to 290 K, indicating a more complete collapse and shielding of all atoms especially the hydrophobic groups from water. Contact probabilities between all atom types and water show significant decrease between 280 K and 320 K. Between 280 K and 320K, the contact

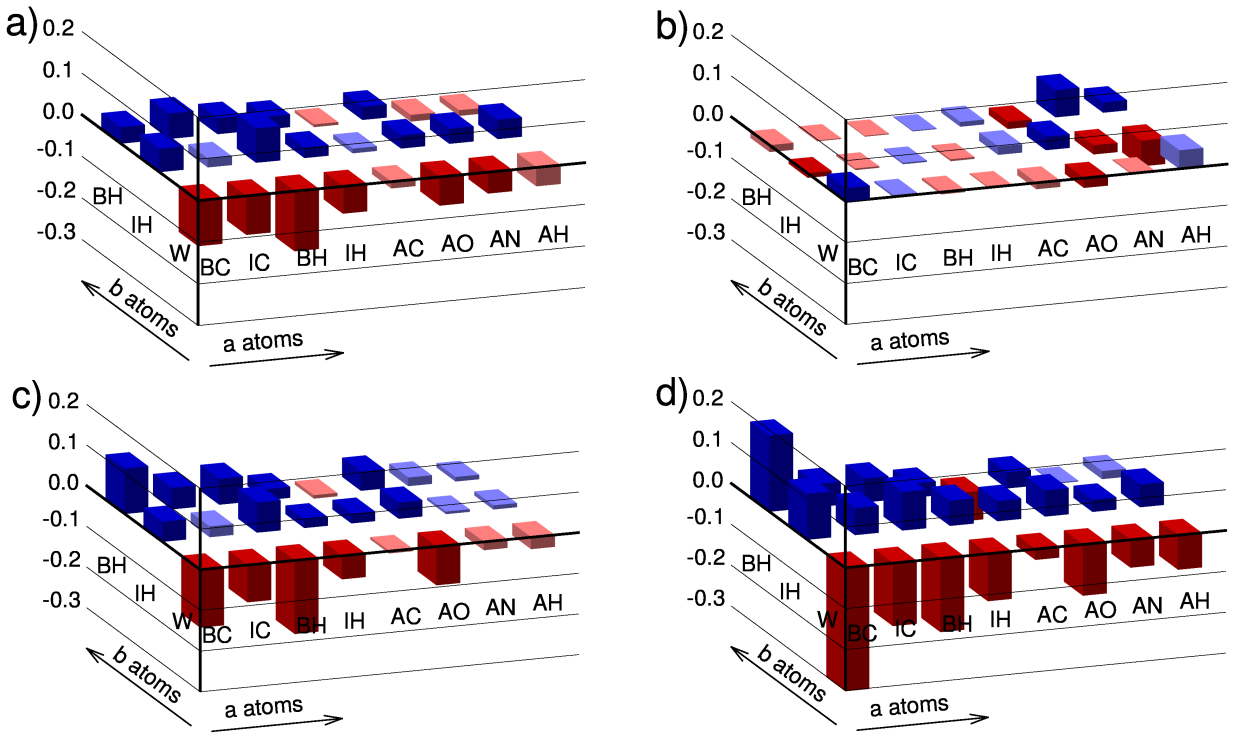

Figure 3: Highlighted portions of the full Voronoi analysis. a: $\Delta\langle p_{ab}\rangle$, 280 K compact - 280 K extended. b: $\Delta\langle p_{ab}\rangle$, 290 K extended - 280 K extended. c: $\Delta\langle p_{ab}\rangle$, 290 K compact - 280 K extended. d: $\Delta\langle p_{ab}\rangle$, 320 K compact - 280 K extended. Each bar is the $\Delta\langle p_{ab}\rangle$ between the extended chain at 280 K and the other states. The rows ranging from left to right represent the a atoms and the columns extending into the page represent the b atoms. Blue indicates a positive $\Delta\langle p_{ab}\rangle$. Red indicates a negative $\Delta\langle p_{ab}\rangle$. The dark bars are statistically significant changes. Atom types are abbreviated according to Figure 2: BC is backbone carbon, IC is isopropyl carbon, BH is backbone hydrogen, IH is isopropyl hydrogen, AC is amide carbon, AO is amide oxygen, AN is amide nitrogen, AH is amide hydrogen, and W is water.

probabilities increase between most atom types and hydrophobic hydrogens. The interactions between the amide atoms and water decrease more strongly between 290 K and 320 K than between 280 K and 290 K, especially amide hydrogen and water indicating that they dehydrate only in the later stages of the transition.

To investigate the amide group interactions with water in further detail, we examine the intermolecular hydrogen bonds, i.e between amide groups and water. Hydrogen bonds are measured using standard geometric criteria of $d < 3.0$ Å and $\theta > 130°$, with d being the donor–acceptor distance and θ – donor–hydrogen–acceptor angle, respectively. The number of hydrogen bonds, N_{HB}, for the entire polymer chain is calculated throughout the simula-

tions, the per monomer contributions of amide group acting both as donor and acceptor are shown at 3 temperatures for different oligomer conformations in Figure S2 in the SI. Figure S2 shows that extended polymer configurations have higher N_{HB} and higher contact probabilities with water than collapsed states from the BRW Voronoi analysis. Backbone-water contacts are more sensitive to the swelling state compared to the residue-water contacts.

There is a notable difference between the different hydrogen bond contact statistics, amide oxygen–water and amide hydrogen–water, during the transition: data from the full Voronoi analysis shows 76.0% of the total (280 K - 320 K) drop in contact probability between amide hydrogen and water occurs between 290 K and 320 K, compared to 34.4% for amide oxygen and water. This correlates with the hydrogen bonds: 68.1% of the total (280 K - 320 K) drop in hydrogen bonds between amide hydrogen and water occurs between 290 K and 320 K, compared to 41.6% between 290 K and 320 K (See Figure S2 in SI). Analysis of the number of water molecules in the first solvation shell and of the solvent–accessible surface area show similar results (See Figure S3).

In summary, the extended state at 280 K is similarly well hydrated as the extended state at 290 K. This good solvation is a further indication of the existence of a long–lived metastable state: a free–energy barrier to de–solvation has to be overcome before the free energy can be lowered when reaching a collapsed state. An unambiguous determination of the globally stable state is therefore not possible based on these atomistic simulations. Clearly either coarse–grained simulations or a free energy technique would be necessary. This means that many, if not all, simulations for conformational transitions reported in the literature have likely been too short to obtain the conclusions that have been stated.

Because of the notably very long equilibration times necessary, we performed direct phase equilibrium simulations as discussed by Gubbins[43] and Köddermann et al. for polymeric systems.[27] To make this feasible in an atomistic model, we studied short ONIPAM chains (trimers) in water. Experimentally, short oligomers have a higher LCST than longer chains.[44,45] Recently, this trend was confirmed by studying NIPAM oligomers as short as

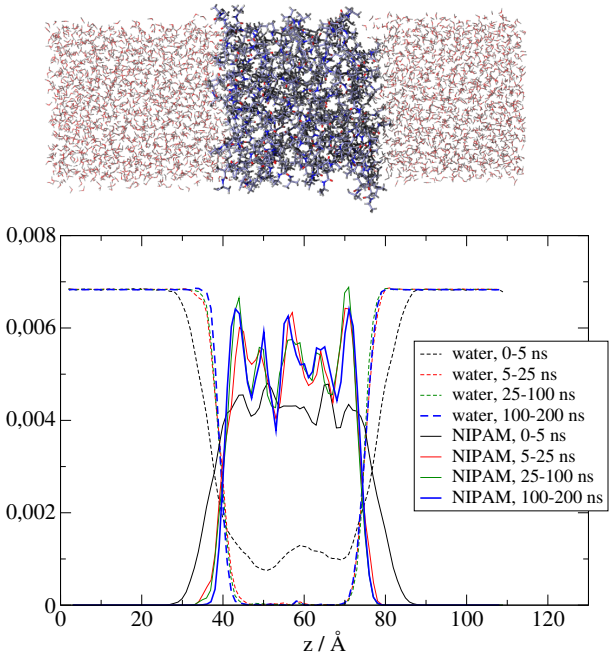

Figure 4: Top: Snapshot of the simulation box of 80 Amber94 NIPAM trimers in 3200 TIP3P water molecules at 280 K after 200 ns. Hydrogen atoms are depicted in grey, oxygen ones in red, carbon ones in iceblue and nitrogen ones in blue. Bottom: density profiles of NIPAM units and water (the latter divided by 5) in a mixture of NIPAM trimers and water at 280 K started from an already inhomogeneous density distribution.

Table 1: List of potential models evaluated and the systems that have been studied with them. X: used, —: not used.

Potential model(s)	Used for the simulaiton of				
	1 30mer in water	72 10mers in water	80 3mers in water	20 3mers in water	125 2mers in water
OPLS–AA[8,9] and SPC/E[13]	X	X	X	X	—
OPLS–AA[8,9] and TIP3P[14]	—	—	X	X	—
amber94[24] and TIP3P[14]	—	—	X	X	—
G45A3[35] and SPC/E[13]	—	—	—	—	X
PCFF[22,23]	—	—	—	X	—

10 monomers.[46] Therefore, if trimers exhibit a phase separation at a given temperature, it is safe to assume that longer chains modeled with the same potential phase separate from water at the same T as well. Initial simulations of 20 trimers distributed randomly in 800 water molecules develop inhomogeneities within 5–10 ns for all potential combinations studied (OPLS–AA + SPC/E and TIP3P; Amber94 + TIP3P; Gromos45A3 + SPC/E; PCFF,

cf. Table 1) at 280 K. OPLS–AA + SPC/E was also studied at 260 K and shows the same results, albeit with much slower kinetics. However, often more than one NIPAM cluster forms and the clusters remain separated and stable for over 100 ns, i.e. they neither dissolve nor unite to a clearly separated polymer phase indicating again that either longer or larger simulations are needed. Therefore, we investigated larger systems with 80 trimers and 3200 water starting from an inhomogeneous density distribution. In Figure 4 one can see that the ONIPAM–rich phase dehydrates further within the first 25 ns of the simulations and that in the last 175 ns, there is a pure water phase in equilibrium with a pure NIPAM phase at 280 K. The other systems studied (OPLS–AA + SPCE and TIP3P) exhibit similar dehydration but the polymer–rich phase still contains some water after $200 - 250$ ns (see SI) such that a complete phase separation is not realized. For OPLS–AA + SPC/E simulations with larger systems using 72 decamers distributed homogeneously in 25584 water molecules have been performed and yield a pure water phase and aggregated chains as well within 200 ns (see Figure S4).

Conclusion

Our simulation results show that the conformational transition of a 30mer of NIPAM can take much longer than anticipated in literature. For most systems, except very short oligomer chains at low concentration, the observation of such a transition is out of reach of atomistic MD and free energy techniques and/or coarse–graining are needed.

On the other hand, all studied combinations of potentials (cf. Table 1) produce a separation of NIPAM oligomers and water into phases with low mutual miscibility at 280 K (or even 260 K) and 320 K. We see clear dehydration of the chains with increasing temperature. Simulations at lower temperatures are not possible because of prohibitively slow kinetics. That means the potentials either do not lead to an LCST at all or do so only at much lower temperatures than observed experimentally (305 K). The results demonstrate a clear

need for a force field that can describe the NIPAM water system correctly. It is possible that simple two–body potentials with standard combining rules are not able to reproduce this system reliably and special interactions between hetero–atoms which are not directly an average of the homo interaction have to be taken into account. We have preliminary indications that such an approach could be successful. As alternatives more involved models including three–body interactions, polarizability or quantum–effects could to be used.

Because of the slow kinetics, no final conclusion can be obtained on whether the conformational transition of a 30mer is indicative of the LCST of a macroscopic system but many studies from the literature clearly used too short simulation times.

Acknowledgement

The authors thank the Deutsche Forschungsgemeinschaft for support within SFB 985 "Functional microgels and microgel systems" as well as the University of California–National Laboratory Labfee Program (grant number 237353). We also thank the IT center of RWTH Aachen University for providing computational resources under grant rwth0068.

Supporting Information Available

Results for additional force fields and system sizes, initial geometries of all used molecules and all used force–field parameters can be found in the supporting information.

This material is available free of charge via the Internet at `http://pubs.acs.org/`.

References

(1) Ward, M. A.; Georgiou, T. K. Thermoresponsive Polymers for Biomedical Applications. *Polymers* **2011**, *3*, 1215–1242.

(2) Pelton, R. Temperature-sensitive Aqueous Microgels. *Adv Colloid Interface Sci* **2000**, *85*, 1–33.

(3) Scherzinger, C.; Schwarz, A.; Bardow, A.; Leonhard, K.; Richtering, W. Cononsolvency of Poly-N-isopropyl Acrylamide (PNIPAM): Microgels versus Linear Chains and Macrogels. *Curr Opin Coll Interface Sci* **2014**, *19*, 84–94.

(4) Walter, J.; Ermatchkov, V.; Vrabec, J.; Hasse, H. Molecular Dynamics and Experimental Study of Conformation Change of Poly(N-isopropylacrylamide) Hydrogels in Water. *Fluid Phase Equilibr.* **2010**, *296*, 164–172.

(5) Lee, S. G.; Pascal, T. A.; Koh, W.; Brunello, G. F.; Goddard III, W. A.; Jang, S. S. Deswelling Mechanisms of Surface-Grafted Poly(NIPAAm) Brush: Molecular Dynamics Simulation Approach. *J. Phys. Chem. C* **2012**, *116*, 15974–15985.

(6) Alaghemandi, M.; Spohr, E. Molecular Dynamics Investigation of the Thermo-Responsive Polymer Poly(N-isopropylacrylamide). *Macromol. Theor. Simul.* **2012**, *21*, 106–112.

(7) Deshmukh, S. A.; Sankaranarayanan, S. K. R. S.; Suthar, K.; Mancini, D. C. Role of Solvation Dynamics and Local Ordering of Water in Inducing Conformational Transitions in Poly(N-isopropylacrylamide) Oligomers through the LCST. *J. Phys. Chem. B* **2012**, *116*, 2651–2663.

(8) Jorgensen, W. L.; Tirado-Rives, J. The OPLS [Optimized Potentials for Liquid Simulations] Potential Functions for Proteins, Energy Minimizations for Crystals of Cyclic Peptides and Crambin. *J. Am. Chem. Soc.* **1988**, *110*, 1657–1666.

(9) Jorgensen, W. L.; Maxwell, D. S.; Tirado-Rives, J. Development and Testing of the OPLS All-Atom Force Field on Conformational Energetics and Properties of Organic Liquids. *J. Am. Chem. Soc.* **1996**, *118*, 11225–11236.

(10) van Gunsteren, W.; Billeter, S.; Eising, A.; Hünenberger, P.; Krüger, P.; Mark, A.; Scott, W.; Tironi, I. Biomolecular Simulation: The Gromos 96 Manual and User Guide. vdf Hochschulverlag AG an der ETH Zürich, Zürich, Switzerland.

(11) Oostenbrink, C.; Villa, A.; Mark, A. E.; van Gunsteren, W. F. A Biomolecular Force Field Based on the Free Enthalpy of Hydration and Solvation: The GROMOS Force-Field Parameter Sets 53A5 and 53A6. *J. Comput. Chem.* **2004**, *25*, 1656–1676.

(12) van Gunsteren, W.; Berendsen, H. Gromos-87 Manual. Biomos BV Nijenborgh 4, 9747 AG Groningen, The Netherlands, 1987.

(13) Berendsen, H. J. C.; R., G. J.; Straatsma, T. P. The Missing Term in Effective Pair Potentials. *J. Phys. Chem.* **1987**, *91*, 6269–6271.

(14) Jorgensen, W. L.; Chandrasekhar, J.; Madura, J. D.; Impey, R. W.; Klein, M. L. Comparison of Simple Potential Functions for Simulating Liquid Water. *J. Chem. Phys.* **1983**, *79*, 926–935.

(15) Vanegas, J. M.; Longo, M. L.; Faller, R. Crystalline, Ordered and Disordered Lipid Membranes: Convergence of Stress Profiles due to Ergosterol. *J. Am. Chem. Soc.* **2011**, *133*, 3720–3723.

(16) Sodt, A. J.; Sandar, M. L.; Gawrisch, K.; Pastor, R. W.; Lyman, E. The Molecular Structure of the Liquid-Ordered Phase of Lipid Bilayers. *J. Am. Chem. Soc.* **2014**, *136*, 725–732.

(17) Liu, M. S.; Taylor, C.; Chong, B.; Liu, L.; Bilic, A.; Terefe, N. S.; Stockmann, R.; Thang, S. H.; De Silva, K. Conformational Transitions and Dynamics of Thermal Responsive Poly(N-isopropylacrylamide) Polymers as Revealed by Molecular Simulation. *Europ Polym J* **2014**, *55*, 153–159.

(18) Tucker, A. K.; Stevens, M. J. Study of the Polymer Length Dependence of the Single Chain Transition Temperature in Syndiotactic Poly(N-isopropylacrylamide) Oligomers in Water. *Macromolecules* **2012**, *45*, 6697–6703.

(19) Abbott, L. J.; Tucker, A. K.; Stevens, M. J. Single Chain Structure of a Poly(N-isopropylacrylamide) Surfactant in Water. *J. Phys. Chem. B* **2015**, *119*, 3837–3845.

(20) Mayo, S. L.; Olafson, B. D.; Goddard III, W. A. DREIDING: A Generic Force Field for Molecular Simulations. *J. Phys. Chem.* **1990**, *94*, 8897–8909.

(21) Levitt, M.; Hirshberg, M.; Sharon, R.; Laidig, K. E.; Daggett, V. Calibration and Testing of a Water Model for Simulation of the Molecular Dynamics of Proteins and Nucleic Acids in Solution. *J. Phys. Chem. B* **1997**, *101*, 5051–5061.

(22) Sun, H.; Mumby, S. J.; Maple, J. R.; Hagler, A. T. An ab Initio CFF93 All-Atom Force Field for Polycarbonates. *J. Am. Chem. Soc.* **1994**, *116*, 2978–2987.

(23) Sun, H. Ab Initio Calculations and Force Field Development for Computer Simulation of Polysilanes. *Macromolecules* **1995**, *28*, 701–712.

(24) Cornell, W. D.; Cieplak, P.; Bayly, C. I.; Gould, I. R.; Merz, K. M., Jr.; Ferguson, D. M.; Spellmeyer, D. C.; Fox, T.; Caldwell, J. W.; Kollman, P. A. A Second Generation Force Field for the Simulation of Proteins, Nucleic Acids, and Organic Molecules. *J. Am. Chem. Soc.* **1995**, *117*, 5179–5197.

(25) Francis, R.; Jijil, C. P.; Prabhu, C. A.; Suresh, C. H. Synthesis of Poly(N-isopropylacrylamide) Copolymer Containing Anhydride and Imide Comonomers - A Theoretical Study on Reversal of LCST. *Polymer* **2007**, *48*, 6707–6718.

(26) Wu, C.; Wang, X. Globule-to-Coil Transtion of a Single Homopolymer Chain in Solution. *Phys. Rev. Lett.* **1998**, *80*, 4092–4094.

(27) Köddermann, T.; Kirschner, K. N.; Vrabec, J.; Hülsmann, M.; Reith, D. Liquid-liquid Equilibria of Propylene Glycol Dimethyl Ether and Water by Molecular Dynamics. *Fluid Phase Equilibr.* **2011**, *310*, 25–31.

(28) Plimpton, S. J. Fast Parallel Algorithms for Short-Range Molecular Dynamics. *J. Comput. Phys.* **1995**, *117*, 1–19.

(29) Jewett, A. I.; Zhuang, Z.; Shea, J.-E. Moltemplate a Coarse-Grained Model Assembly Tool. *Biophys. J.* **2013**, *104*, 169a.

(30) Humphrey, W.; Dalke, A.; Schulten, K. VMD - Visual Molecular Dynamics. *J Molec Graphics* **1996**, *14*, 33–38.

(31) Martínez, L.; Andrade, R.; Birgin, E. G.; Martínez., J. M. Packmol: A package for Building Initial Configurations for Molecular Dynamics Simulations. *J. Comput. Chem.* **2009**, *30*, 2157–2164.

(32) Nosé, S. A Unified Formulation for the Constant Temperature Molecular-Dynamics Methods. *J. Chem. Phys.* **1984**, *81*, 511–519.

(33) Hockney, R.; Goel, S.; Eastwood, J. Quiet High-Resolution Computer Models of a Plasma. *J. Comput. Phys.* **1974**, *14*, 148 – 158.

(34) Ryckaert, J.-P.; Cicotti, G.; Berendsen, H. J. C. Numerical Integration of the Cartesian Equations of Motion of a System with Constraints: Molecular Dynamics of n-alkanes. *J. Comput. Phys.* **1977**, *23*, 327–341.

(35) Lukas, D.; Daura, X.; van Gunsteren, W. An Improved GROMOS96 Force Field for Aliphatic Hydrocarbons in the Condensed Phase. *J. Comput. Chem.* **2001**, *22*, 1205–1218.

(36) Pronk, S.; Páll, S.; Schulz, R.; Larsson, P.; Bjelkmar, P.; Apostolov, R.; Shirts, M.; Smith, J.; Kasson, P.; van der Spoel, D.; Hess, B.; Lindahl, E. GROMACS 4.5: A High-throughput and Highly Parallel Open Source Molecular Simulation Toolkit. *Method. Biochem. Anal.* **2013**, *29*, 845–854.

(37) Bussi, G.; Donadio, D.; Parrinello, M. Canonical Sampling through Velocity Rescaling. *J. Chem. Phys.* **2007**, *126*, 014101.

(38) Parrinello, M.; Rahman, A. Polymorphic Transitions in Single Crystals: A New Molecular Dynamics Method. *J. Appl. Phys.* **1981**, *52*, 7182–7190.

(39) Essmann, U.; Perera, L.; Berkowitz, M. L.; Darden, T.; Lee, H.; Pedersen, L. G. A Smooth Particle Mesh Ewald Potential. *J. Chem. Phys.* **1995**, *103*, 8577–8592.

(40) Hess, B.; Bekker, H.; Berendsen, H. J. C.; Fraaije, J. G. E. M. LINCS: A Linear Constraint Solver for Molecular Simulations. *J. Comput. Chem.* **1997**, *18*, 1463–1472.

(41) Isele-Holder, R.; Rabideau, B.; Ismail, A. Definition and Computation of Intermolecular Contact in Liquids Using Additively Weighted Voronoi Tessellation. *J. Phys. Chem. A* **2012**, *116*, 4657–4666.

(42) Rycroft, C. Voro++: A three-dimensional Voronoi cell library in C++. *Chaos* **2009**, *19*, 041111.

(43) Gubbins, K. E. The Role of Computer Simulation in Studying Fluid Phase Equilibria. *Mol. Simulat.* **1989**, *2*, 223–252.

(44) Schild, H. G.; Tirrell, D. A. Microcalorimetric Detection of Lower Critical Solution Temperatures in Aqueous Polymer Solutions. *J. Phys. Chem.* **1990**, *94*, 4352–4356.

(45) Tong, Z.; Zeng, F.; Zhang, X.; Sato, T. Inverse Molecular Weight Dependence of Cloud Points for Aqueous Poly(N-isopropylacrylamide) Solutions. *Macromolecules* **1999**, *32*, 4488–4490.

(46) Kather, M.; Pich, A. Synthesis and Claud Point Determination of monodisperse NIPAM Oligomers consting of 10 to 71 monomers. Personal Communication, 2016.

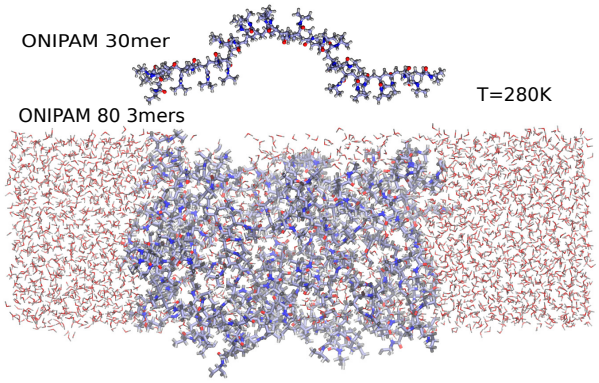
ONIPAM 30mer
T=280K
ONIPAM 80 3mers